

## An investigation of stress-strain behavior of FRP-confined concrete under cyclic compressive loading

R. Abbasnia\*, A. Holakoo

Received: January 2011, Revised: August 2011, Accepted: November 2011

### Abstract

One important application of fiber reinforced polymer (FRP) is to confine concrete as FRP jackets in seismic retrofit process of reinforced concrete structures. Confinement can improve concrete properties such as compressive strength and ultimate axial strain. For the safe and economic design of FRP jackets, the stress-strain behavior of FRP-confined concrete under monotonic and cyclic compression needs to be properly understood and modeled. According to literature review, it has been realized that although there are many studies on the monotonic compressive loading of FRP-confined concrete, only a few studies have been conducted on the cyclic compressive loading. Therefore, this study is aimed at investigating the behavior of FRP-confined concrete under cyclic compressive loading. A total of 18 cylindrical specimens of FRP-confined concrete were tested in uniaxial compressive loading with different wrap thickness, and loading patterns. The results obtained from the tests are presented and examined; based on analysis of test results predictive equations for plastic strain and stress deterioration were derived. The results are also compared with those from two current models, comparison revealed the lack of sufficient accuracy of the current models to predict stress-strain behavior and accordingly some provisions should be incorporated.

*Keywords:* Confined concrete, Stress-strain behavior, Fiber reinforced polymer, Cyclic loading

### 1. Introduction

In recent years, the use of FRP has increased significantly mainly due to the high strength-to-weight ratio, tensile strength and elastic modulus. Experience of past earthquakes has demonstrated that one of the main weak points of reinforced concrete structures can be assigned to the lack of ductility of reinforced concrete beam-columns. One possible method to increase strength and ductility is to confine these structural elements by use of FRP confinement. For the safe and economic design of FRP jackets, the stress-strain behavior of FRP-confined concrete under monotonic and cyclic compression needs to be properly understood and modeled.

Therefore, several models have been presented for the evaluation of stress-strain behavior of FRP-confined concrete. Most of current models are based on monotonic compressive loading [5-18] and only a few studies have been carried out on cyclic compressive loading [19-27, 35-37]. Largely due to the increasing importance of seismic analysis, the need for further

research on cyclic compressive loading can be identified at various levels of analysis.

To the best of author's knowledge, only two models have been proposed thus far for cyclic stress-strain behavior. Shao et al [25] studied plastic strains; strength and stiffness deterioration on the basis of experimental works and proposed a model for cyclic compressive loading without considering the effect of loading history. Lam and Teng [27] presented predictive equations for stress deterioration, plastic strain and unloading and reloading paths with consideration of loading history using the obtained results from their own and other studies. They also suggested a model for predicting the stress-strain behavior of FRP-confined concrete under cyclic compressive loadings.

The accuracy of current models in some cases such as investigating the effect of cyclic loading on ultimate strength and strain of FRP-confined concrete, and the effect of repeated unloading/reloading cycles on stress-strain behavior is not satisfying [26]. Therefore, in this study the behavior of FRP-confined concrete under monotonic and cyclic (unloading/reloading cycles) compressive loading has been studied through an experimental program and the accuracy of the current models have been compared with that of the test results.

\* Corresponding Author: [abbasnia@iust.ac.ir](mailto:abbasnia@iust.ac.ir)  
Department of Civil Engineering, Iran University of Science and Technology, Tehran, Iran

## 2 Experimental works

### 2.1 Test specimens

In this study, 18 concrete cylinders with diameter and height of 152mm×305 mm have been constructed and categorized into two series (I, II). The first series were wrapped with 2 and the second series with 3 plies made of carbon fiber reinforced polymer (CFRP). Also, 8 unconfined concrete specimens were prepared as control specimens.

All specimens were made of the same batch of concrete. CFRP jackets were formed in a wet lay-up process by wrapping three discrete carbon fiber sheets with the impregnation of epoxy resin. For each layer of FRP, an overlap length of 150 mm was provided to form a vertical joint [28]. Epoxy resins for the CFRP consisted of two components, namely the main component and the hardener. The weight ratio of the components was 100:38, respectively. The specimens were labeled with letters L, C and M in two groups of LpCq-r and LpM-r, where p is the number of layers, q is the number of cycles per unloading and reloading, and r is the specimen number. L, M and C stand for “layer”, “monotonic compressive loading” and “cyclic compressive loading”, respectively (Table 1).

### 2.2 Strain gauge layout

Longitudinal shortenings were measured using two linear variable differential transducers (LVDT) locating at 180° from each other and covering the mid-height region of 20cm (Fig.1(b)). Hoop strains were measured using 4 strain gauges with the gauge length of 20 mm. One of them was installed at overlapping region and the remaining was installed out of the region with the interval of 90° in the mid-height of the specimen. Figure 1 shows the test setup and the location of the strain gauges.

**Table 1.** Loading pattern

Specimens Series	Loading pattern	Specimen label
I	Monotonic	L2M-1
		L2M-2
		L2M-3
	Single cycle at prescribed displacements	L2C1-1
		L2C1-2
		L2C1-3
Three repeated cycles at prescribed displacements	L2C3-1	
	L2C3-2	
	L2C3-3	
II	Monotonic	L3M-1
		L3M-2
		L3M-3
	Single cycle at prescribed displacements	L3C1-1
		L3C1-2
		L3C1-3
Three repeated cycles at prescribed displacements	L3C3-1	
	L3C3-2	
	L3C3-3	

### 2.3 CFRP properties

CFRP sheets are used for these experiments were two-way fiber (woven fabrics). Nominal thickness and strength of each layer are 0.26 mm and 4200 MPa, respectively. The nominal thickness was used in the calculation of material properties. To obtain FRP composite properties, standard tensile specimens were prepared according to the ASTM-D3039 [29]. Tensile test was conducted on 6 FRP composite specimens, 3 of which were with 2 plies and the others with 3 plies. On the basis of the results, the average rupture stress of 2 and 3 plies were 780 and 787 MPa, respectively. The properties of CFRP and epoxy resin and also the results of tensile tests on the CFRP composites are summarized in table 2.

### 2.4 Compressive test

Loading was applied by a 3000 KN MTS testing machines under displacement control at a constant rate of 1 mm/min. For 8 controlling and 3 confined concrete specimens of each

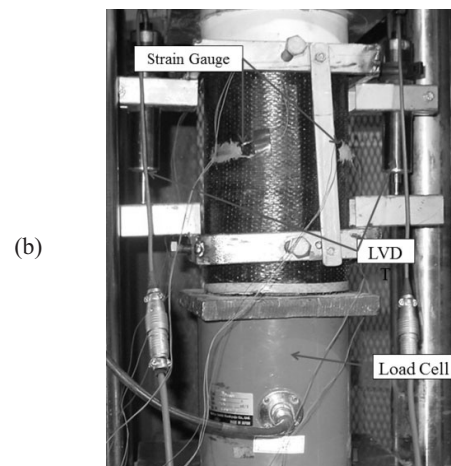
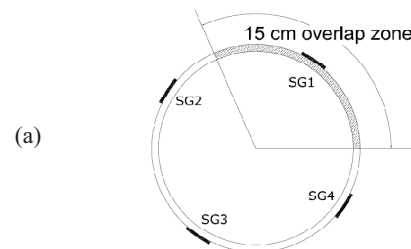


**Fig. 1.** (a) Strain gauges layout; (b) test specimen

**Table 2.** Material properties

	CFRP	Epoxy resin	2-ply CFRP composite	3-ply CFRP composite
Nominal thickness (mm)	0.26	---	0.52	0.78
Ultimate stress (MPa)	4210	71	780	787
Elastic modulus (GPa)	230	3550	---	---
Ultimate strain (%)	1.82	2.5	---	---

series, compressive load was applied with monotonically increasing displacements until failure occurred. The failure of confined concrete in all specimens was in the form of sudden rupture of FRP jacket. For the remaining 12 FRP-confined specimens, cyclic compressive loading including unloading and reloading cycles was performed.

Three specimens of each series were subjected to a single loading/unloading cycle at each prescribed displacement level. In this case, the specimens were loaded by increasing the axial displacement to a prescribed value, and were next unloaded by reducing the axial displacement to a target load level. The specimens were then reloaded to the next prescribed displacement. The rest of the specimens were subjected to 3 unloading/reloading cycles at each prescribed unloading displacement level. For both cases of cyclic compression, the target load level at which unloading was terminated and reloading started was lower than 20 KN.

### 3 Test results

The compression tests of the unconfined concrete cylinders showed that the concrete had an unconfined compressive strength  $f_{co}$  of 46.3 MPa.

All the FRP-confined specimens failed by the rupture of FRP jacket. The results of tests are shown in Table 3. In this table ultimate axial strain is the average of two axial LVDT results. The average rupture hoop strain was calculated by taking from the average values of 4 installed strain gauges. According to the tests observations, the maximum hoop strain was located outside of overlapping zone and in the vicinity of the specimen failure point.

#### 3.1 Stress-strain curves

Stress-strain curves of unconfined and FRP-confined concrete are shown in Fig. 2. As it is shown in this figure,

**Table 3.** CFRP Specimens test results

Specimen name	Ultimate strength $\sigma_{cu}$ (MPa)	Ultimate axial strain, $\epsilon_{cu}$	CFRP hoop rupture strain $\epsilon_{h,rup}$	
			Average	Maximum
L2M-1	54.7	0.007168	0.007253	0.012145
L2M-2	56.4	0.006789	0.005808	0.01033
L2M-3	61.6	0.006039	0.008371	0.01069
L2C1-1	56.7	0.006157	0.007474	0.008722
L2C1-2	56.2	0.007817	0.007417	0.010223
L2C1-3	58.9	0.007167	0.007943	0.009736
L2C3-1	50.7	0.006546	0.006348	0.010138
L2C3-2	53.7	0.006285	0.006985	0.010475
L2C3-3	50.4	0.007123	0.007184	0.011184
L3M-1	67.2	0.009409	0.008242	0.010532
L3M-2	64.7	0.007736	0.007819	0.0111
L3M-3	67.5	0.007652	0.006782	0.008237
L3C1-1	62.1	0.008738	0.00959	0.011751
L3C1-2	66.5	0.007602	0.007011	0.009601
L3C1-3	70.2	0.00836	0.006957	0.008199
L3C3-1	69.1	0.008593	0.007549	0.009777
L3C3-2	66.3	0.008729	0.008704	0.010396
L3C3-3	67.8	0.00894	0.008203	0.009988

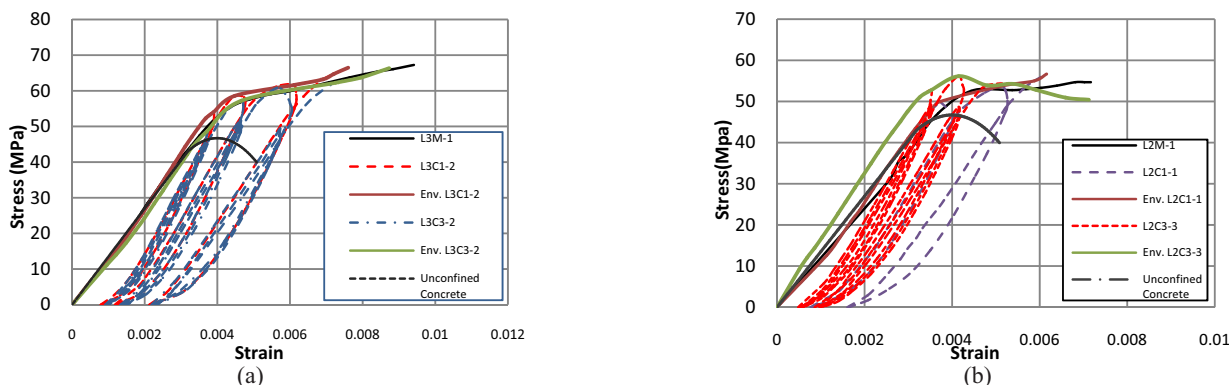


**Fig. 2.** Stress-strain curves, (a) 3-ply CFRP specimens; (b) 2-ply CFRP specimens

the initial portion of stress-strain curve of the unconfined and FRP-confined concrete is approximately similar.

As it is shown in Fig. 2, while the shape of reloading path was linear, the unloading path was nonlinear and a residual strain remained in the specimens at zero stress. Due to the formation of internal cracks in the concrete and strength degradation, reloading path does not return to the initial unloading stress and reaches to a rather lower stress value. Repeated unloading/reloading cycles have a cumulative effect on stress deterioration and plastic strain.

Comparisons between monotonic and cyclic envelope curve in Fig. 2 (a) and (b) show that the envelope curve of the cyclic compressive loading is entirely above the monotonic loading curve. This is in agreement with the finding of the studies by Rodriguez and Silva [19, 20], Lam and Teng [26].

### 3.2 Rupture strain in CFRP

The results of different studies have indicated that confined concrete failure occurs after FRP rupture. Ultimate axial stress and strain occurs when the strain of FRP reaches to the ultimate rupture limit. Lam and Teng [26] showed that FRP rupture strain in FRP-confined concrete was less than that of obtained from FRP composite tensile test. They attributed their observations to the following three reasons a) the curvature of FRP jacket, b) the non-uniform deformation of cracked concrete, and c) overlapping zone.

The maximum hoop strain during the failure of CFRP is presented in Table 3. Maximum hoop strain of each specimen is lower than that of the carbon fiber provided by the manufacturer in Table 2. The average of the maximum strains of Table 3 is 1.02% which is 56% lower than the carbon fiber strain.

The hoop strains measured at the CFRP failure point are shown in Fig. 3. Due to higher thickness, the hoop strain of FRP in the overlapping zone is lower than that of in the outside of this zone.

Comparison between rupture strains for specimens under cyclic and monotonic loading in Fig. 4 revealed that the amount of rupture strain due to cyclic loading is greater than that of monotonic loading in some specimens and is less than the other specimens. This means that cyclic compressive loading has no significant effect on the FRP rupture strains.

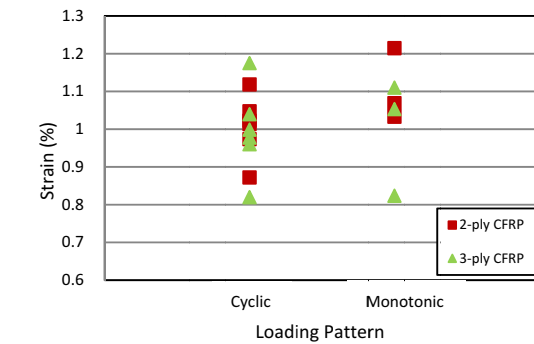
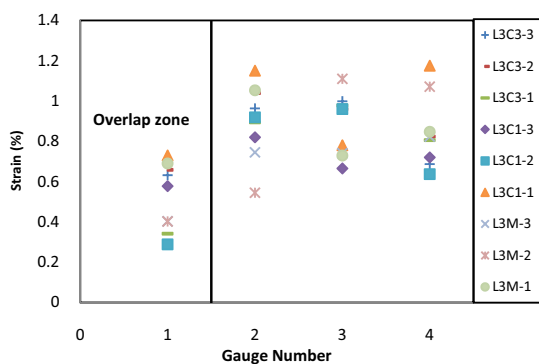


Fig. 4. Comparison between cyclic and monotonic rupture strain

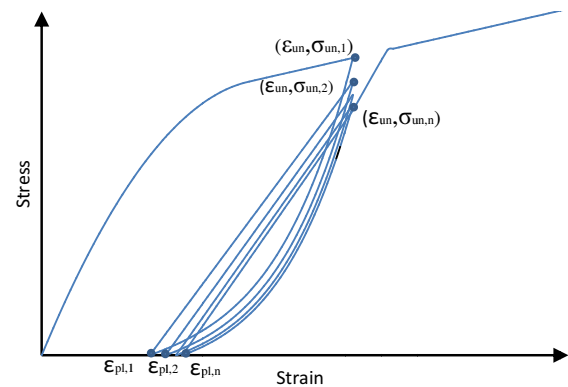


Fig. 5. Key parameters of cyclic stress-strain curves

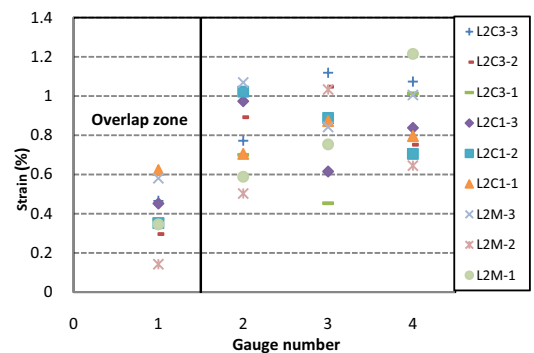


Fig. 3. Hoop strains measured at the CFRP failure point on (a) 3-ply specimens; (b) 2-ply specimens

### 3.3 Effect of unloading/reloading cycles on the stress-strain diagram

According to Karsan and Jirsa research [2], repeated unloading/reloading cycles (loading history) have a cumulative effect on the plastic strain and stress deterioration. Fig. 5 schematically shows the parameters considered in this section.  $\epsilon_{un}$  is the strain at the starting point of unloading.  $\sigma_{un}$  and  $\epsilon_{pl,n}$  are the stress at starting of nth unloading cycle and plastic strain at nth unloading/reloading cycle, respectively.

#### 3.3.1 Investigation of Plastic strain

The plastic strain is defined as the residual axial strain of concrete when it is unloaded to zero stress. The results of

previous studies indicated the existence of a linear relation between plastic strain in the first unloading stage ( $\epsilon_{pl,1}$ ) and unloading strain. Thus, the unloading process was stopped prior to reaching the point of zero stress. In the current paper, to calculate the plastic strain, the unloading curve was extended by nonlinear regression to the zero stress. A plot of plastic strain versus unloading strain is shown in Fig. 6. From linear regression of experimental results of 2 and 3-ply specimens, Eq. 1 is proposed to predict plastic strain

$$\epsilon_{pl,1}(\epsilon_{un} \geq 0.0035) = 0.6976\epsilon_{un} - 0.0018 \quad (1)$$

Where,  $\epsilon_{un}$  and  $\epsilon_{pl,1}$  are unloading strain and plastic strain in the first unloading stage, respectively.

Sakai and Kawashima [4] introduced a ratio to study the effect of loading history on the plastic strains. This ratio called increasing strain ratio  $\gamma_n$  is defined as follows

$$\gamma_n = \frac{\epsilon_{un} - \epsilon_{pl,n}}{\epsilon_{un} - \epsilon_{pl,n-1}} \quad (n \geq 2) \quad (2)$$

Values of  $\gamma_n$  for 2nd and 3rd cycles are shown in Fig.7. The linear relation between  $\gamma_n$  and number of cycles,  $n$ , are thus presented as Eq. 3

$$\gamma_n(\epsilon_{un} \geq 0.0035) = 0.0169n + 0.9341 \quad (2 \leq n \leq 3) \quad (3)$$

### 3.3.2 Investigation of stress deterioration

According to the previous studies [19-27], after each unloading and reloading cycle, the stress corresponding to the initial unloading strain deteriorated to a stress lower than the preceding cycle. In order to evaluate the effect of loading history on strain deterioration, Sakai and Kawashima [4]

proposed the ratio  $\beta_n$ . This ratio is described by Eq.4

$$\beta_n = \frac{\sigma_{un,n+1}}{\sigma_{un,n}} \quad (4)$$

Where,  $\sigma_{un,n}$  is unloading stress in the nth cycle and  $\sigma_{un,n+1}$  is the stress corresponding to unloading strain on the nth reloading path.

The stress deterioration versus,  $n$  obtained from these tests results, is cited in Fig 8. It can be seen that by increasing  $n$ , the stress deterioration ratio increase, and the level of confinement have little effect on the stress deterioration. The linear relation between  $\beta_n$  and  $n$ , are thus presented as Eq. 5

$$\beta_n(\epsilon_{un} \geq 0.0035) = 0.00317n + 0.894 \quad (1 \leq n \leq 3) \quad (5)$$

Based on the test results, Eq. 3 and Eq. 5 are applicable for unloading strains  $\epsilon_{un}$  ranging from 0.0035 and ultimate strain. For unloading strains outside this range, additional tests are required.

### 3.4 Comparisons of the test results with other experiments

Many studies have examined the behavior of FRP-confined concrete under uniaxial compression. Fig.9 shows a comparison between results of the present tests and the experimental results obtained in other investigations [11, 25, 28, 30-34]. In Fig. 9(a) comparison between hoop strains versus confinement ratio (CR) are shown. Confinement ratio is defined as the ratio of confined stress  $f_r$ , to unconfined strength  $f'_{co}$  of concrete and given by Eq. 6

$$CR = \frac{f_r}{f'_{co}} = \frac{E_{frp} \epsilon_{h,rup} t_{frp}}{f'_{co} R} \quad (6)$$

where  $E_{frp}$  is the elastic modulus of the FRP,  $\epsilon_{h,rup}$  hoop strain of the FRP,  $t$  nominal thickness of the FRP and  $R$  radius of the specimen. As it is shown in Fig. 9(a) for the hoop strain in the range of 0.8 to 1.2 %, the results of present study are in good agreement with the results of other researches [11, 25, 28, 30-34]. Comparison between confined concrete strength ratios ( $\sigma_{cu}/f'_{co}$ ) versus confinement ratio are shown in Fig. 9(b). As it is shown in this figure confined concrete strength ratio has linear relation with confinement ratio and results of present test follow this linear relation. In Fig. 9(c) comparison between stress deterioration ratio versus confinement ratio for first unloading cycle are shown, as it is shown stress deterioration have wide range (0.8 to 0.97).

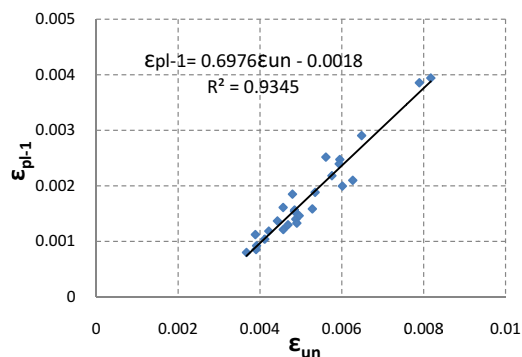


Fig. 6. Plastic strains versus unloading strains

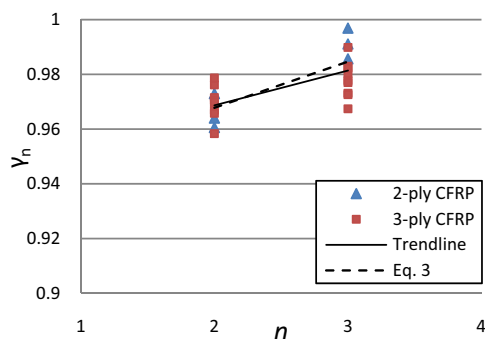


Fig. 7. Increasing strain ratio versus number of effective cycles

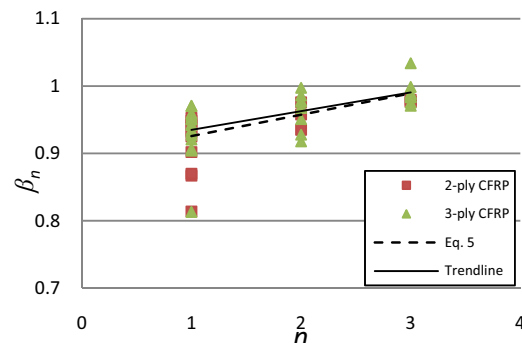


Fig. 8. Stress deterioration ratio versus number of effective cycles

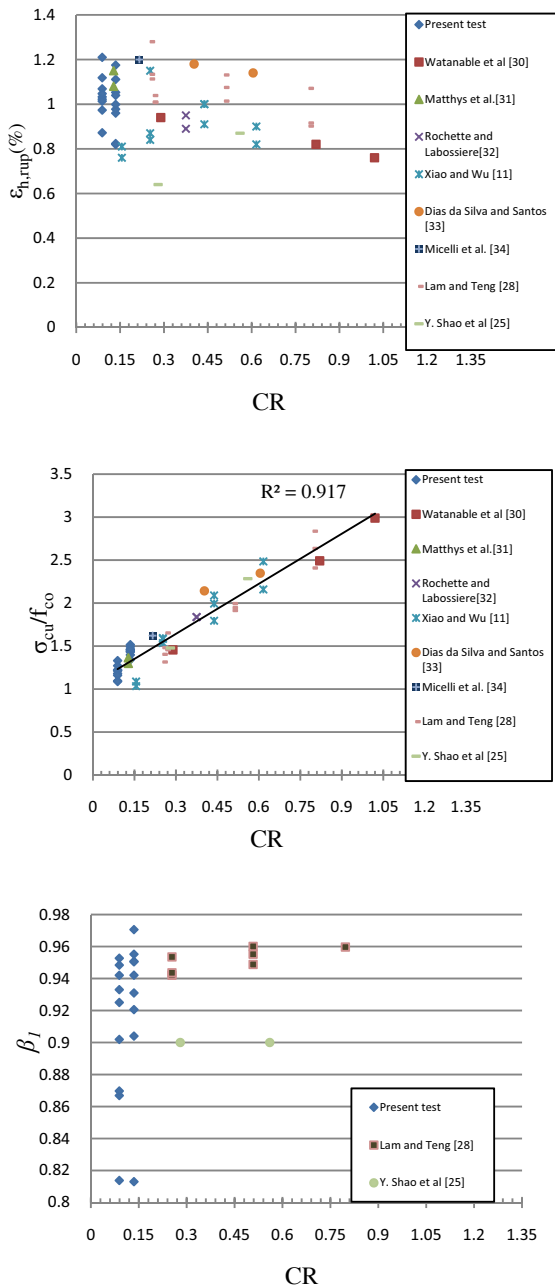


Fig. 9. (a) hoop strain versus confinement ratio (CR), (b) confinement strength ratio versus CR, (c) stress deterioration ratio versus CR

#### 4 Comparison of the test results with the current stress-strain models

This section deals with the analysis of the existing stress-strain models by Shao et al [25] and Lam and Teng [27]. Since the Shaomodel does not consider the effect of loading history, the specimens with single loading cycle have been selected for comparison. Lam and Teng [27] developed their model for the effect of loading history for maximum 5 repeated cycles. For the sake of comparison between the obtained result from the Lam and Teng model and present tests, the specimens have been selected with 1 and 3 repeated cycles.

#### 4.1 Shao et al Model [25]

Shao et al [25] presented a model for the compressive unloading and reloading cycles. A more detailed analysis of the model can be found in reference [25]. In this model, the stress-strain model for monotonic behavior proposed by Samaan et al. [6] has been used to predict the envelope curve. They have presented the Eqs. 7 and 8 for the unloading path

$$\sigma_c = \frac{(1-x)^2}{(1+2x)^2} \sigma_{un} \quad (7)$$

Where x defined as Eq. 8

$$x = \frac{\epsilon_c - \epsilon_{un}}{\epsilon_{pl} - \epsilon_{un}} \quad (8)$$

Where, plastic strain is given by Eq. 9

$$\epsilon_{pl} = \epsilon_{un} - \frac{\sigma_{un}}{E_{secu}} \quad (9)$$

is unloading modulus expressed by Eq. 10

$$\frac{E_{secu}}{E_1} = \begin{cases} 1, & 0 \leq \frac{\sigma_{un}}{f'_{co}} < 1 \\ -0.44 \frac{\sigma_{un}}{f'_{co}} + 1.44, & 1 \leq \frac{\sigma_{un}}{f'_{co}} < 2.5 \\ 0.34, & 2.5 \leq \frac{\sigma_{un}}{f'_{co}} \end{cases} \quad (10)$$

Shao et al [25] suggested Eq. 11 for reloading path from the ending of unloading path.

$$\frac{\sigma_{re}}{\epsilon_{re}} = \frac{\sigma_{new}}{\epsilon_{un} - \epsilon_{pl}} \quad (11)$$

$$\sigma_{new} = 0.9 \sigma_{un} \quad (12)$$

Where, is the new stress at the envelope unloading strain.

The strain obtained from the current study has been compared with those obtained from Shao et al model [25], as it is shown in Fig. 10. It can be seen from this figure that, the error of the predicted plastic strains by the model is more than 15 percent. Therefore, plastic strains predicted by Eqs. 8 and 9 are overestimated.

Since the plastic strains predicted by this model were

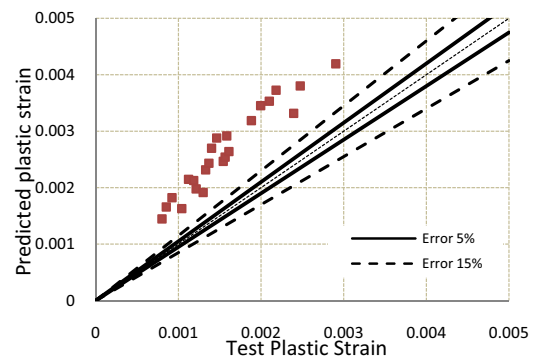


Fig. 10. Prediction of plastic strain using Shao's model

overestimated, the experimental values of plastic strain obtained from the tests were used for a better evaluation of unloading path. Fig. 11 provides a comparison between the results of two specimens of this study and that of the Shao et al model [25]. This comparison shows that the model did not have sufficient accuracy to predict unloading paths but reloading paths match reasonably well.

#### 4.2 Lam and Teng Model [27]

Lam et al. [26] carried out cyclic compressive unloading tests with 3 repeated cycles and they analyzed the unloading history effect on the stress-strain curve. Lam and Teng [27] employed their previous model [17] for envelope loading curve. The unloading curve is expressed by Eq. 13

$$\nu = \frac{\epsilon_{un} - \epsilon_{pl,n}}{\epsilon_{un} - \epsilon_{pl,n-1}} \quad (n > 2) \quad (13)$$

Where, coefficients a, b, c are defined by Eqs. 14-16

$$a = \frac{E_{un,0} - \eta E_{pl}^{\eta-1}}{E_{un,0} - \eta E_{pl}^{\eta-1}} \quad (14)$$

$$\gamma_n (\epsilon_{un} \geq 0.0035) = 0.0169n + 0.9341 \quad (15)$$

$$b = E_{un,0} - \eta E_{pl}^{\eta-1} \quad (15)$$

$$c = -a E_{pl}^{\eta} - b \epsilon_{pl} \quad (16)$$

Where,  $\eta$  and  $\gamma_n$  are controlling exponent and unloading path secant at zero stress point respectively, and are expressed in Eqs. 17 and 18.

$$\eta = 350 \epsilon_{un} + 3 \quad (17)$$

$$E_{un,0} = \min \left\{ \begin{array}{l} \frac{0.5 f'_{co}}{\epsilon_{un}} \\ \frac{\sigma_{un}}{\epsilon_{un} - \epsilon_{pl}} \end{array} \right. \quad (18)$$

The reloading curve consists of linear and parabolic portions. The first one covers from the reloading strain to initial unloading strain and the second one covers from the initial unloading strain to envelope curve.

The linear part is described by Eq. 19.

$$\sigma_c = \sigma_{re} + E_{re} (\epsilon_c - \epsilon_{re}), \quad (\epsilon_{re} \leq \epsilon_c \leq \epsilon_{ref}) \quad (19)$$

Where, the slope of linear portion can be determined from Eq. 20.

$$E_{re} = \frac{\sigma_{new} - \sigma_{re}}{\epsilon_{ref} - \epsilon_{re}}, \quad (\epsilon_{re} \leq \epsilon_c \leq \epsilon_{ref}) \quad (20)$$

The parabolic portion is expressed as follows (Eq. 21)

$$\sigma_c = A \epsilon_c^2 + B \epsilon_c + C, \quad (\epsilon_{ref} \leq \epsilon_c \leq \epsilon_{ret,env}) \quad (21)$$

They suggested Eqs. 22 to 24 for predicting  $\gamma_n$  and  $\beta_n$  respectively

$$\epsilon_{pl,1} = (0.87 - 0.004 f'_{co}) \epsilon_{un} - 0.0016 \quad 0.0035 \leq \epsilon_{un} \leq \epsilon_{cu} \quad (22)$$

$$\gamma_n = 0.0212n + 0.88 \quad 0.0035 \leq \epsilon_{un} \leq \epsilon_{cu} \quad (23)$$

$$\beta_n = 0.013n + 0.925 \quad \epsilon_{un} \geq 0.002 \quad (24)$$

They mentioned that Eqs. 23 and 24 are applicable when  $\epsilon_{un} \geq 0.0035$ . Further information can be found in reference [27].

The plastic strains obtained from the test are presented in comparison with the Lam and Teng model, as shown in Fig. 12. It is apparent that the plastic strains predicted by Lam and Teng model are overestimated.

Figure 13 shows the comparison between the results obtained from the tests and the model. In predicting unloading curve experimental values of plastic strain  $\epsilon_{pl}$  were used, because the

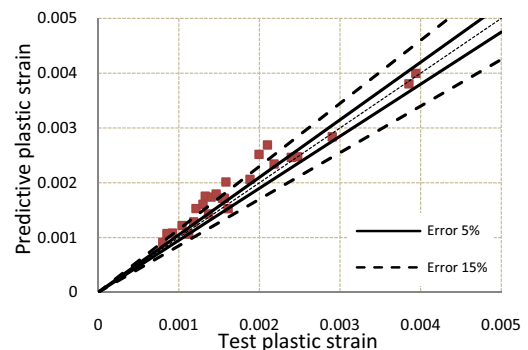


Fig. 12. Prediction of plastic strain using Lam and Teng model

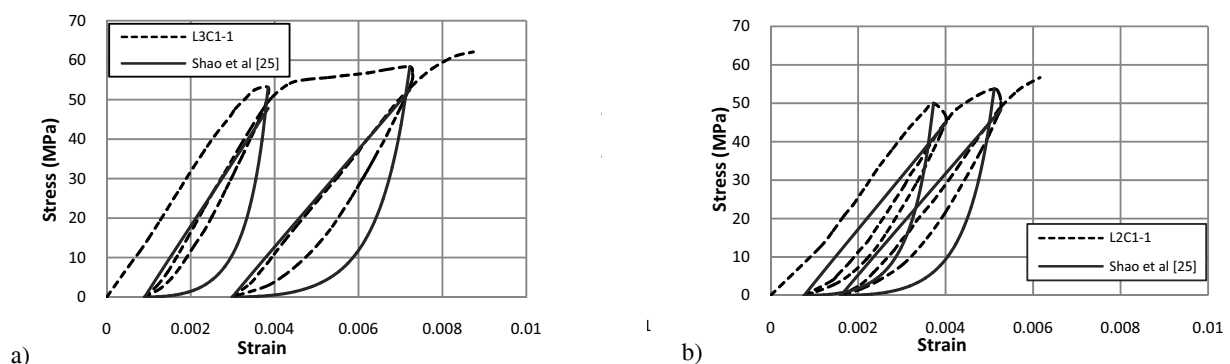


Fig. 11. (a) and (b) Comparison between Shao's model and test results

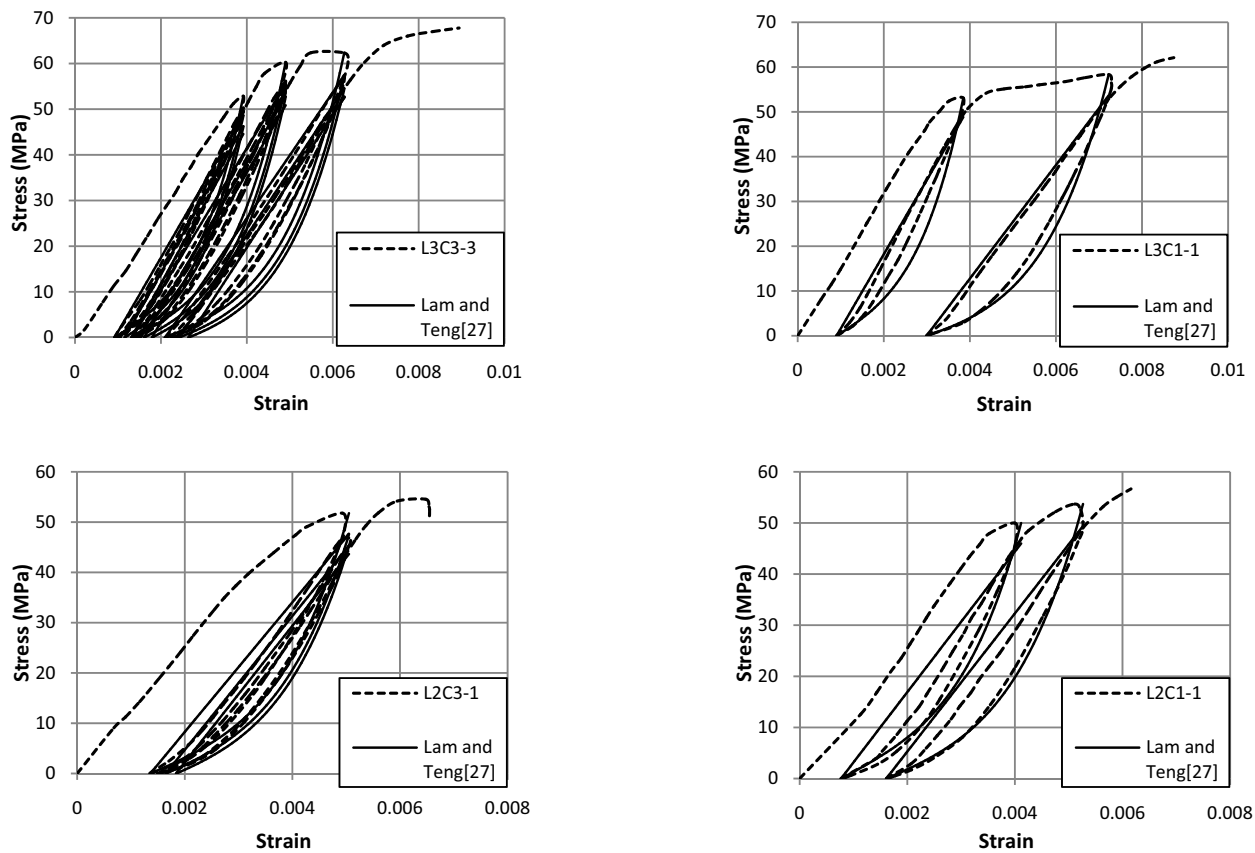


Fig. 13. Comparison between Lam and Teng model and test results

use of Eq. 22 overestimate the plastic strain. As it is shown, the model gave the unloading/reloading paths in specimens with single unloading/reloading cycle with a favorable accuracy. In specimens with three repeated unloading/reloading cycle, first unloading/reloading curve match the test results reasonably well, but in next cycles do not. This can be assigned to the lack of accuracy in the predicting of increasing strain ratio, and stress deterioration.

## 5 Conclusions

In this study a total of 18 CFRP-confined concrete cylindrical specimens were tested in uniaxial compression under monotonic and cyclic compressive loading. The test variables which considered in this study included thickness of the FRP sheet and loading patterns. The results obtained from the cyclic compression tests on the CFRP-confined concrete cylinders have been presented and discussed. Predictive equations have been proposed for determining the plastic strain and stress deterioration on the basis of regression analysis of the test results. Moreover, the test results have been compared with those from two cyclic stress-strain models for FRP-confined concrete. From the analytical and experimental results, the following conclusions can be drawn:

Unloading/reloading cycles have negligible effect on the envelope curve of stress-strain behavior of CFRP-confined concrete.

Cyclic loading has no significant effect on the CFRP jacket rupture strain.

Comparison between the test results and Shao model [25] indicated that this model shows favorable performance in the prediction of reloading path, but it has a limited accuracy to predict unloading path.

Comparison of the test results and Lam and Teng model [27] indicated that the proposed unloading/reloading paths match the test results reasonably well. But it does not have sufficient accuracy to predict plastic strains and stress deterioration.

## 7 References

- [1] Sinha BP, Gerstle KH, Tulin LG.: 1964, Stress-strain relations for concrete under cyclic loading, *ACI J.* 61(2), 195–211.
- [2] Karsan ID, Jirsa JO.: 1969, Behavior of concrete under compressive loadings, *J. Structural Eng. Div. ASCE*, 95(ST12), 2543–2563.
- [3] Bahn BY, Hsu CTT.: 1998, Stress-strain behavior of concrete under cyclic loading, *ACI Mater. J.*, 95(2), 178–192.
- [4] Sakai J, Kawashima K.: 2006, Unloading and reloading stress-strain model for confined concrete, *J. Structural Eng. ASCE*, 132(1), 112–122.
- [5] Karbhari VM, Gao Y.: 1997, Composite jacketed concrete under uniaxial compression-verification of simple design equations, *J. Mater. Civil Eng. ASCE*, 9(4), 185–193.
- [6] Samaan M, Mirmiran A, Shahawy M.: 1998, Model of concrete confined by fiber composite, *J. Structural Eng. ASCE*, 124(9), 1025–1031.
- [7] Miyauchi K, Inoue S, Kuroda T, Kobayashi A.: 1999, Strengthening effects of concrete columns with carbon fiber sheet, *Trans. Japan Conc. Inst.*, 21, 143–150.



- [8] Saafi M, Toutanji HA, Li Z.: 1999, Behavior of concrete columns confined with fiber reinforced polymer tubes, *ACI Mater. J.*, 96(4), 500–509.
- [9] Spoelstra MR, Monti G.: 1999, FRP-confined concrete model, *J. Compos. Const. ASCE*, 3(3), 143–150.
- [10] Toutanji HA.: 1999, Stress–strain characteristics of concrete columns externally confined with advanced fiber composite sheets, *ACI Mater. J.*, 96(3), 397–404.
- [11] Xiao Y, Wu H.: 2000, Compressive behavior of concrete confined by carbon fiber composite jackets, *J. Mater. Civil Eng. ASCE*, 12(2), 139–146.
- [12] Xiao Y, Wu H.: 2003, Compressive behavior of concrete confined by various types of FRP composite jackets, *J.Reinf.Plast.Compos.*, 22(13), 1187–1202.
- [13] Fam AZ, Rizkalla SH.: 2001, Confinement model for axially loaded concrete confined by circular fiber reinforced polymer tubes, *ACI Structural J.*, 98(4), 451–461.
- [14] Teng JG, Lam L.: 2002, Compressive behavior of carbon fiber reinforced polymer-confined concrete in elliptical columns, *J. Structural, Eng. ASCE*, 128(12), 1535–1543.
- [15] Lam L, Teng JG.: 2002, Strength models for fiber reinforced plasticconfined concrete, *J. Structural Eng. ASCE*, 128(5), 612–623.
- [16] Lam L, Teng JG.: 2003, Design-oriented stress–strain model for FRPconfined concrete, *Const. Build Mater.*, 17(6–7), 471–489.
- [17] Lam L, Teng JG.: 2003, Design-oriented stress–strain model for FRPconfined concrete in rectangular columns, *J. Reinf. Plast. Compos.*, 22(13), 1149–1186.
- [18] Mirmiran A, Shahawy M.: 1997, Behavior of concrete columns confined by fiber composites, *J. Structural Eng. ASCE*, 123(5), 583–590.
- [19] Rodrigues CC, Silva MG.: 2001, Experimental investigation of CFRP reinforced concrete columns under uniaxial cyclic compression. Proceedings, fifth international conference on fibre-reinforced plastics for reinforced concrete structures, London U.K. Thomas Telford, 783–792.
- [20] Rodrigues CC, Silva MG.: 2001, The behavior of GFRP reinforced concrete columns under monotonic and cyclic axial compression, *Composites in constructions*, proceedings of the international conference, Lisse, The Netherlands: A.A. Balkema Publishers, 245–250.
- [21] Theodoros R.: 2001, Experimental investigation of concrete cylinders confined by carbon FRP sheets, under monotonic and cyclic axial compression load, Research Report. Publication 01:2, Division of Building Technology, Chalmers University of Technology.
- [22] Ilki A, Kumbasar N.: 2002, Behavior of damaged and undamaged concrete strengthened by carbon fiber composite sheets, *J. Structural Eng. Mechanic*, 13(1), 75–90.
- [23] Ilki A, Kumbasar N.: 2003, Compressive behavior of carbon fiber composite jacketed concrete with circular and non-circular cross sections, *J. Earthquake Eng.*, 7(3), 381–406.
- [24] Shao Y.: 2003, Behavior of FRP-confined concrete beam-columns under cyclic loading, PhD Thesis, North Carolina State University, USA.
- [25] Shao Y., Zhu Z., Mirmiran A.: 2006, Cyclic modeling of FRP-confined concrete with improved ductility, *J. Cem.Concr.Compos.*, 28, 959–968.
- [26] Lam L, Teng JG, Cheung JG, Xiao Y.: 2006, FRP-confined concrete under axial cyclic compression, *J.Cem.Concr. Compos.*, 28(10), 949–958.
- [27] Lam L, Teng JG.: 2008, Stress–strain model for FRP-confined concrete under cyclic axial compression, *J. Engineering Structures.*
- [28] Lam L, Teng JG.: 2004, Ultimate condition of fiber reinforced polymer confined concrete, *J. Compos. Const. ASCE*, 8(6), 539–548.
- [29] American Society for Testing and Materials (ASTM): 1995, Standard test method for tensile properties of polymer matrix composites materials, Annual book of ASTM standards, ASTM D3039/D3039M–95, Vol. 14.02.
- [30] Watanabe K, Nakamura H, Honda T, Toyoshima M, Iso M, Fujimaki T, et al.: 1997, Confinement effect of FRP sheet on strength and ductility of concrete cylinders under uniaxial compression., *Non-Metallic (FRP) Reinforcement for Concrete Structures*, Proceedings of the Third International Symposium, vol. 1, Sapporo, Japan: Japan Concrete Institute, 233–240.
- [31] Matthys S, Taerwe L, Audenaert K.: 1999, Tests on axially loaded concrete columns confined by fiber reinforced polymer sheet wrapping., *Proceedings of the Fourth International Symposium on Fiber Reinforced Polymer Reinforcement for Reinforced Concrete Structures*, SP-188, Farmington, Michigan, USA: American Concrete Institute, 217–229.
- [32] Rochette P, Labossiere P.: 2000, Axial testing of rectangular column models confined with composites., *J Compos Constr*, ASCE;4(3):129–36.
- [33] Dias da Silva V, Santos JMC.: 2001, Strengthening of axially loaded concrete cylinders by surface composites., *Composites in Constructions*, Proceedings of the International Conference, Lisse, The Netherlands: A.A. Balkema Publishers, 257–262.
- [34] Micelli F, Myers JJ, Murthy S.: 2001, Effect of environmental cycles on concrete cylinders confined with FRP., *Composites in Constructions*, Proceedings of the International Conference, Lisse, The Netherlands: A.A. Balkema Publishers, 257–262.
- [35] Sharbatar M.K.: 2008, Monotonic and cyclic loading of new FRP reinforced concrete cantilever beams, *International Journal of Civil Eng.*, 6(1), 58–71
- [36] Eshghi S., Zanjani Zadeh V.: 2007, Repair of Earthquake-Damaged Square R/C Columns with Glass Fiber-Reinforced Polymer, *International Journal of Civil Eng.*, 5(3), 210–223
- [37] Abbasnia R., Ziaadini H.: 2009, Behavior of concrete prisms confined with FRP composites under axial cyclic compression, *Engineering Structures*, 32(3), 648–655